atmosphere

MDPI

Article

Representing Ozone Formation from Volatile Chemical Products (VCP) in Carbon Bond (CB) Chemical Mechanisms

Greg Yarwood * and Katie Tuite

Ramboll, 7250 Redwood Boulevard, Suite 105, Novato, CA 94945, USA; ktuite@ramboll.com
* Correspondence: gyarwood@ramboll.com

Abstract: Volatile organic compound (VOC) emissions to the atmosphere cause air pollution associated with adverse health outcomes. Volatile chemical products (VCPs) have emerged as a VOC emission category that is poorly characterized by air pollution models. VCPs are present throughout developed economies in manufactured products that include paints, cleaning agents, printing inks, adhesives and pesticides. Air quality models must accurately represent the atmospheric chemistry of VCPs to develop reliable air quality plans. We develop a chemical mechanism for oxidant formation by VCP compounds that is compatible with version 6 of the Carbon Bond (CB6) mechanism. We analyzed a recent U.S. VCP emission inventory and found that ~67% of the emissions mass can be well-represented by existing CB6 mechanism species but ~33% could be better represented by adding 16 emitted VCP species including alcohols, ethers, esters, alkanes and siloxanes. For larger alkanes, an important VCP category, our mechanism explicitly represents temperature-dependent organic nitrate formation and autoxidation via 1,6 H-shift reactions consistent with current knowledge. We characterized the ozone forming potential of each added VCP species and compared it to the current practice of representing VCP species by surrogate species. Nine of the sixteen added VCP species are less reactive than the current practice, namely i-propanol, dimethyl ether, methyl formate, ethyl formate, methyl acetate, larger esters, i-butane, large alkanes and siloxanes. These less reactive VCP species are characterized by having OH-reactions that form un-reactive products. A total of 7 of the 16 VCP species are more reactive than current practice, namely n-propanol, ethylene glycol, propylene glycol, larger alcohols, diethyl ether, larger ethers and ethyl acetate. These more reactive VCP species are characterized as containing functional groups that promote faster OH-reaction. The VCP chemical mechanism for CB6 can improve how VCP impacts to oxidants are represented and will be incorporated to CB7. Changes in oxidant formation resulting from the mechanism update will depend on how VCP emissions are speciated for modeling, which is uncertain, and impacts may go in opposite directions for specific categories of VCP emissions that have unique chemical speciation characteristics. We provide guidance to help modelers implement the VCP mechanism update.

Keywords: VCP; volatile chemical product; ozone; VOC reactivity; chemical mechanism; Carbon Bond; CB6; CAMx

Citation: Yarwood, G.; Tuite, K. Representing Ozone Formation from Volatile Chemical Products (VCP) in Carbon Bond (CB) Chemical Mechanisms. *Atmosphere* **2024**, *15*, 178. https://doi.org/10.3390/atmos15020178

Academic Editors: Le Cao and Xuewei Hou

Received: 27 December 2023
Revised: 29 January 2024
Accepted: 30 January 2024
Published: 31 January 2024

1. Introduction

Emissions of volatile organic compounds (VOCs) to the atmosphere cause air pollution of ozone (O_3) and fine particulate matter with a diameter smaller than 2.5 µm ($PM_{2.5}$), which are associated with adverse human health impacts worldwide [1,2]. Many human activities lead to anthropogenic VOC emissions including fossil fuel production, fuel combustion, industrial processes, and using VOC-containing products for domestic and commercial purposes, which makes establishing accurate emission inventories challenging [3–5]. VOC-containing products are increasingly referred to as "volatile chemical products" (VCPs) by the air quality community, and, as a category VCPs, include solvents, paints, printing inks, adhesives, pesticides, cleaning agents and personal care products [6,7]. Efforts to control U.S anthropogenic VOC emissions and improve urban air quality have

been most successful for emission categories that are identifiably important and amenable to regulation, notably on-road mobile sources, leaving a growing contribution of VCPs to anthropogenic VOC emissions [1,2]. Many VCPs contain organic compounds that are engineered and manufactured to improve product performance and, in some cases, facilitate air quality management strategies to reduce overall VOC emissions, e.g., transitioning from solvent-based to water-based surface coatings [8]. Engineered VOCs (e.g., ether-alcohol solvents, and siloxanes) are chemically distinct from traditional VOCs refined from crude oil (e.g., alkanes and aromatics) and therefore behave differently in the atmosphere [6,7,9,10]. We refer to these engineered VOCs as VCP compounds to differentiate them from traditional VOC compounds. The importance of VCP emissions is illustrated by the U.S. EPA 2016 emission inventory for the continental U.S. wherein solvent emissions of 2.6 million tons/year contribute about 20% of total anthropogenic VOC emissions [5].

Chemical transport models (CTMs) are essential tools for understand non-linear relationships between VOC emissions and O_3/$PM_{2.5}$ pollution and conducting air quality planning [1,2,11–13]. Atmospheric oxidants, especially hydroxyl radical (OH), are central to atmospheric photochemistry in the troposphere [14], and the chemical reactions oxidants, VOCs and other air pollution precursors such as nitrogen oxides (NOx) are described by chemical mechanisms [15]. For efficiency, CTMs rely upon condensed chemical mechanisms [15] rather than near-explicit chemical mechanisms such as the Master Chemical Mechanism (MCM), which has $>10^4$ reactions of $>10^3$ species [16]. The Carbon Bond (CB) condensed chemical mechanisms [17–20] are included in the Community Multiscale Air Quality (CMAQ) model [21] and the Comprehensive Air quality Model with extensions (CAMx) CTM [22], which are widely used [11,12], and other atmospheric models [23,24].

Here, we develop a condensed chemical mechanism for oxidant formation from VCP compounds that is compatible with version 6 series CB mechanisms (CB6). Our motivation is to support improved representation of VCP emissions in air quality modeling and planning. We analyze a recent (2019) U.S.-wide VCP emission inventory [25] and identify 16 VCP species to include in our VCP mechanism. Some of these VCP mechanism species are "lumped", meaning designed to represent families of similar compounds, and modelers need to know how to map specific VCP compounds from emission inventories to our VCP mechanism species, a process we refer to as mapping [26]. We provide recommendations for mapping emission inventory compounds to our VCP mechanism species.

2. Methodology

We identify VCP compounds to be represented in our VCP chemical mechanism by analyzing a recent VCP emission inventory of the U.S. that is being incorporated into U.S Environmental Protection Agency (EPA) emission inventories for air quality planning [5]. We evaluate how well this VCP emission inventory is represented by existing CB6 mechanism species and the potential for improvement by using 16 new VCP mechanism species. We develop gas-phase chemical mechanisms for OH-radical reactions of the 16 VCP chemical mechanism species. Then, we compare ozone forming potential (OFP) of the VCP chemical mechanism species by computing Maximum Incremental Reactivity (MIR) factors that quantify OFP for conditions where OFP is most strongly sensitive to VOC [27]. In the following text, compound refers to a specific molecule whereas a species is part of a chemical mechanism.

2.1. VCP Emissions Analysis

We use the VCPy [25] U.S.-wide, 2019 emission inventory for VCPs to identify important compounds present in VCP emissions and design the VCP chemical mechanism. VCPy provides a comprehensive inventory of reactive organic carbon (ROC) emissions from sources that include surface coatings, solvents, cleaning products, personal care products and pesticides. Importantly, VCPy resolves estimated total ROC emissions to individual compounds (sometimes groups of similar compounds) by relying on speciation profiles from the U.S. EPA SPECIATE database [28]. Here, speciation profile means the relative

contribution of individual compounds to total emissions for a particular emission category, e.g., water-based printing ink, solvent-based paint, etc. VCPy also includes useful ancillary information for each compound including the molecular weight, estimated vapor pressure, estimated potential SOA-yield, and MIR factor [29].

We combine VCP mass emission estimates by compound from VCPy with ozone MIR factors and SOA-yields, also from VCPy, to compute weighted emission totals by compound. These weighted emission calculations have several uncertainties, including: (1) the source category level ROC emissions reported in VCPy are estimates; (2) assigning total ROC emissions to individual compounds using speciation profiles from SPECIATE is uncertain because the profiles may be incomplete, unrepresentative, or otherwise inaccurate; (3) the available SOA-yield and ozone MIR factors are uncertain and for many compounds present in VCPy they are unavailable, which required assumptions by the VCPy developers to provide a complete database. However, VCPy has the advantages of being comprehensive, current, and relevant to air quality planning because VCPy emission estimates are being used for air quality modeling [5].

To identify important VCP compounds, we tabulated the top-ranked **25** compounds from VCPy by MIR- and SOA-weighted mass (potentially **50** compounds), finding that 11 compounds were present in both rankings, resulting in a list of **39** "top ranked" VCP compounds (Table S1). Reviewing these **39** top-ranked VCP compounds, we found that **21** are well-represented by existing CB6 mechanism species (see Table S1 for details) including several compounds that are explicit in CB6 (methanol, formic acid, ethanol and acetone) plus compounds that have well-established representations using CB6 lumped species (toluene and ethyl benzene represented by TOL; isomers of xylene represented by XYL; and terpenes represented by TERP). The remaining **18** top-ranked VCP compounds are considered "poorly represented" by CB6 and were used to guide the development of the VCP chemical mechanism. Compounds were considered poorly represented when they contain a functional group that is not explicitly represented by an existing CB6 model species, e.g., ethers, esters, alcohols other than methanol/ethanol, and siloxanes. We also considered isobutane and larger alkanes poorly represented because their OH-reaction products are quite different from most alkanes that are represented by CB6 model species PAR (e.g., high acetone yield from isobutane and high organic nitrate yield from larger alkanes).

Contributions of the 18 "poorly represented" VCP compounds to ozone MIR weighted mass and SOA-yield weighted mass are listed in Table S1 and named in Figure 1. Contributions are expressed as a percentage of the total weighted mass summed over all compounds in VCPy (i.e., percentage of total VCP emissions). The **18** compounds fall into 3 groups in Figure 1: (1) compounds with large ozone MIR contribution (>1.5% of total) but small SOA contribution (<0.5%) are alcohols and ethers; (2) compounds with large SOA contribution (>4%) but small ozone MIR contribution (<0.6%) are large alkanes, siloxanes, large esters and Texanol^{TM} (a proprietary ester-alcohol solvent containing 12 C atoms); (3) remaining compounds with relatively small contributions to both ozone MIR (<1.5%) and SOA (<1%). Figure 1 indicates that good separation exists between the top-ranked ozone vs. SOA forming VCP compounds, suggesting that model developers can independently parameterize the oxidant and SOA impacts of VCP emissions within air quality models.

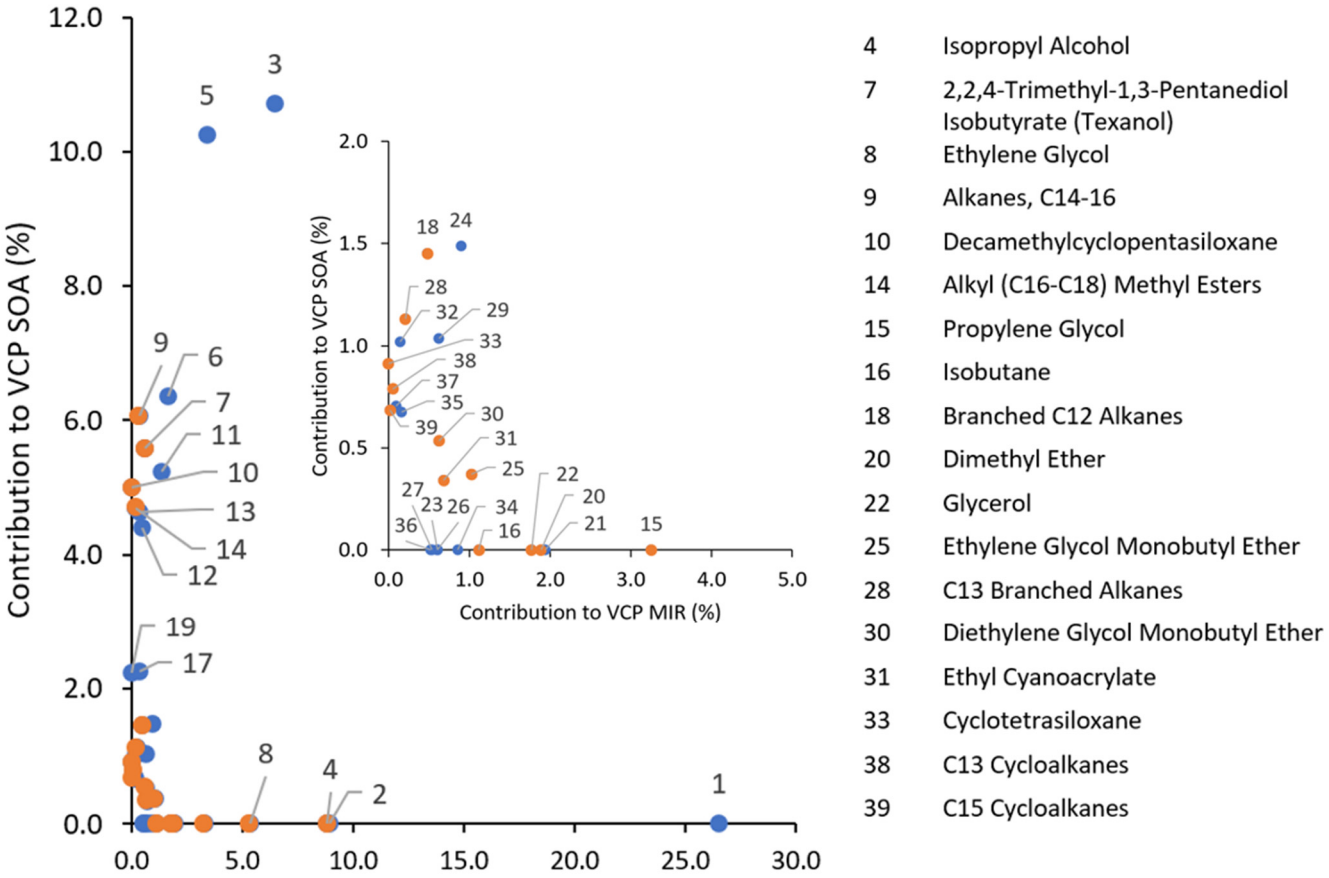

Figure 1. Contributions of the top-ranked compounds to total VCP emissions weighted by ozone MIR and SOA-yield in the 2019 U.S.-wide emission inventory from VCPy. All **39** compound numbers are identified in Table S1, and the **18** compounds considered "poorly represented" are named here and colored orange, whereas **21** "well represented" compounds are colored blue.

2.2. VCPs Selected for Chemical Mechanism Development

Analyzing the VCP emissions, as shown in Figure 1 (and Table S1), identified **18** compounds that rank highly for ozone forming potential and are poorly represented by the existing CB6 mechanism. They can be grouped chemically as follows: alcohols (i-propanol, ethylene glycol and propylene glycol); ethers (dimethyl ether, ethylene glycol monobutyl ether [EGBE] and diethylene glycol monobutyl ether [DEGBE]); esters (2,2,4-Trimethyl-1,3-Pentanediol Isobutyrate [Texanol^{TM}] and alkyl (C16–C18) methyl esters); large alkanes (branched C12 alkanes, C14–16 alkanes, C13 branched alkanes, C13 cycloalkanes, and C15 cycloalkanes), and siloxanes (cyclotetrasiloxane [D4] and decamethylcyclopentasiloxane [D5]). Strategies for developing model compounds to represent these groups are discussed below. Three of the 18 highly ranked compounds fall outside these groups, namely glycerol, i-butane and ethyl cyanoacrylate. We developed an explicit mechanism for i-butane because it has large emissions in VCPy and, as discussed below, forms distinctive degradation products in the atmosphere. We did not develop a chemical mechanism for glycerol (propane-1,2,3-triol) because its large Henry constant (4.7×10^6 mol m^{-3} Pa^{-1}) and relatively low vapor pressure (log C* = 2.86) suggest that condensed-phase reactions will be important for glycerol. We did not develop a chemical mechanism for ethyl cyanoacrylate due to a lack of data.

The VCP mechanism species for which we developed chemical mechanisms are listed in Table 1. There are 19 species in total but 3 (HKET, HPO2, and AUTX) are secondary species, leaving 16 primary species that are intended for representing VCP emissions. For alcohols, ethers and esters, we developed explicit mechanism species to represent the smallest group members that are not already explicit in CB6 (namely IPOH, NPOH,

EDOH, PDOH, DME, DEE, MEFM, ETFM, and ETAC) and lumped mechanism species to represent larger group members (ROH, ETHR, ESTR). Some of the added explicit species are not highly ranked in Figure 1 (NPOH, DEE, MEFM, ETFM, ETAC) but nevertheless mechanisms were developed for completeness. Modelers could choose to implement a subset of these new VCP mechanism species but it should be noted that esters are products of ethers (see their chemical mechanisms below), and, therefore, including an ether species requires also including the dependent ester species. Siloxanes are represented by a single species (SXD5), which consequently is a lumped species, although its chemistry is based on D5 siloxane. Isobutane is treated explicitly (IBTA). Large alkanes are represented by the lumped species HPAR, where the name stands for heavy PAR, by analogy with the CB species PAR, which represents paraffinic carbon. Rules for mapping compounds to HPAR and/or PAR are discussed below. Three new species (HPO2, HKET and AUTX) represent reaction products of HPAR and they are unsuitable for directly representing emitted VCP or other compounds.

Table 1. VCP mechanism species names and properties.

Name	Description	N_C	N_H	N_O	M_r	H^S_{CP}	$H^S_{CP}T$
DEE	Diethyl ether	4	10	1	74.1	11	6600
DME	Dimethyl ether	2	6	1	46.1	7.7	4900
EDOH	1,2-ethanediol (ethylene glycol)	2	6	2	62.1	6.60×10^5	8800
ESTR	Larger esters (C4+, excluding ethyl acetate)	4	7	2	87.1	6	5900
ETAC	Ethyl acetate	4	8	2	88.1	6	5900
ETFM	Ethyl formate	3	6	2	74.1	3.4	4600
ETHR	Larger ethers (C4+, excluding diethyl ether)	4	8	1	72.1	1.1	6600
HKET	Hydroxy-peroxyketone from HPAR	8	16	4	176.2	7700	4600
HPAR	Heavy PAR, based on n-dodecane	12	26		170.3	1.20×10^{-4}	4000
IBTA	2-methylpropane (i-butane)	4	10		58.1	9.20×10^{-4}	2700
IPOH	i-propanol	3	8	1	60.1	130	7500
MEAC	Methyl acetate	3	6	2	74.1	8.1	4900
MEFM	Methyl formate	2	4	2	60.1	4.1	4000
NPOH	n-propanol	3	8	1	60.1	140	6900
PDOH	1,2-propanediol (propylene glycol)	3	8	2	76.1	2.70×10^5	9500
ROH	Larger alcohols (C4+)	4	10	1	74.1	110	7200
SXD5	Siloxanes as D5 (decamethylcyclopentasiloxane)	10	30	5	370.6	3.00×10^{-5}	4000
HPO2	Peroxy radical from HPAR	12	25	3		N/A	
AUTX	Operator for HPO2 autoxidation			2		N/A	

N_C, N_H and N_O are the numbers of C, H and O atoms (species formula). M_r is the relative molar mass (also called molecular weight). H^S_{CP} is the Henry's law solubility constant at 298 K (aq-concentration/partial pressure; dimensionless). H^S_{CP} is the temperature dependence of H^S_{CP} (K, with a default value of 4000 K).

We tested how the combined CB6 and VCP mechanism species represent emissions from VCPy by analyzing the top **200** compounds in the VCPy 2019, U.S.-wide emission inventory. The top **200** compounds were identified by giving equal weighting to emitted mass, ozone MIR weighted mass, and SOA yield weighted mass. Together, the top **200**

compounds accounted for 90.2% of mass, 94.3% of ozone MIR weighted mass and 88.3% of SOA yield weighted mass.

To perform this analysis, we mapped each of the top **200** compounds to CB6 and VCP mechanism species, as shown in Table S2. Figure 2 shows the percentage of carbon mapped to each CB6 and VCP mechanism species, with 67.2% of C mapped to existing CB6 species (including NONR and IVOC) and the remaining 32.8% of C mapped to VCP mechanism species. (Percentage of C can be computed from lumped mechanism species whereas percentage mass cannot). In Figure 2, mechanism species NONR (non-reactive) represents compounds with long atmospheric lifetimes, such as halocarbons, that are not considered as ozone or SOA precursors for regional modeling. The model species IVOC represents intermediate-volatility organic compounds (defined in VCPy as having 3×10^2 μg m^{-3} < C* < 3×10^6 μg m^{-3}) which are not part of CB6 but are treated by many air quality models [21,22,30]. Compounds within the top **200** that are mapped to NONR or IVOC are identified in Table S2 and the methodology for mapping volatile and reactive compounds to VCP and/or CB6 compounds (as in Table S2) is discussed below.

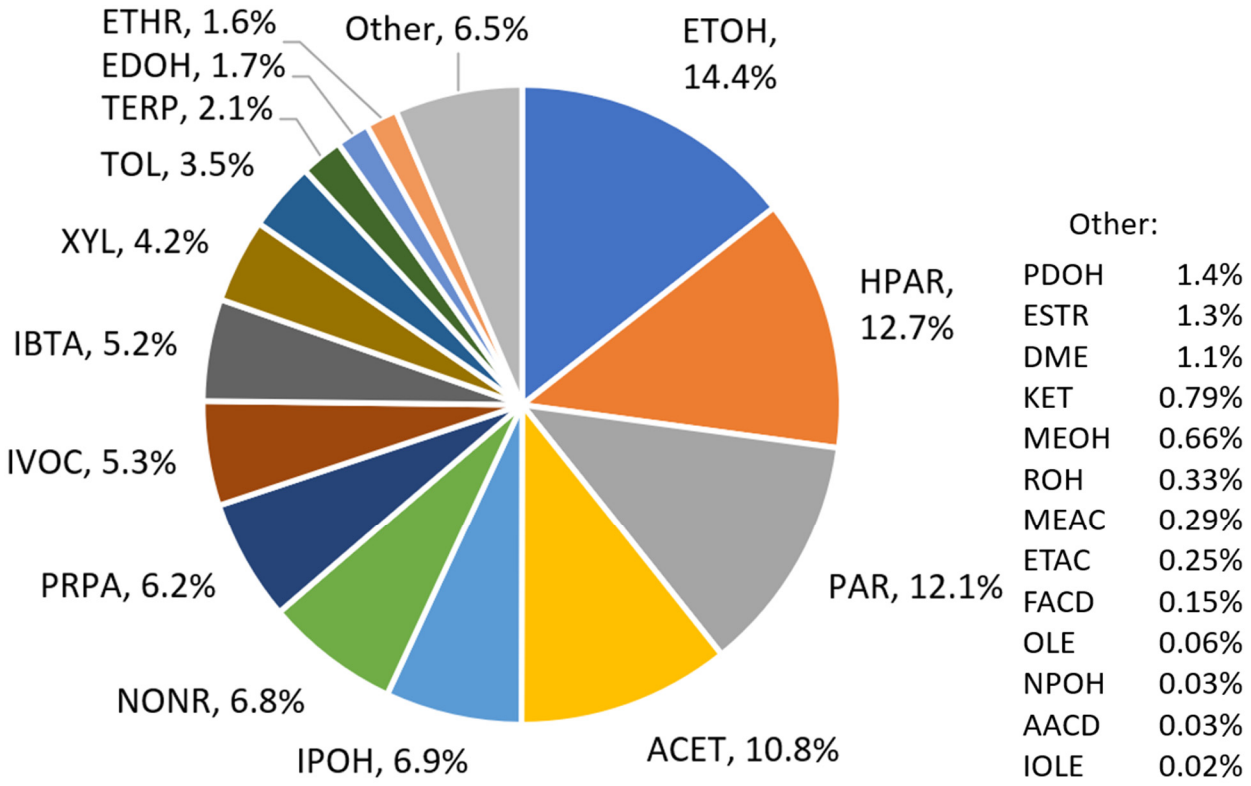

Figure 2. Percentage of carbon mass assigned to individual VCP and CB6 mechanism species from the top **200** ranked compounds in the VCPy 2019 US-wide emission inventory.

From the "top 200" analysis of U.S.-wide VCP emissions (Figure 2), the most heavily utilized VCP mechanism species (Table 1) are HPAR, IPOH, IBTA, ROH and EDOH, with each representing > 1.5% C mass. Notably, the amount of carbon represented by VCP species HPAR (12.7%) and CB6 species PAR (12.1%) is almost equal because large alkanes are prevalent in VCPs. Isopropanol (IPOH) is used in cleaning products, i-butane (IBTA) is an aerosol propellant, and glycols (EDOH and PDOH) are used in water-based formulations as anti-freeze agents and for other reasons [9].

The explicit VCP species NPOH, DEE, MEFM and ETFM do not appear in Figure 2 because neither n-propanol, diethyl ether, methyl formate nor ethyl formate ranked in the top 200. The lumped VCP species SXD5, representing siloxanes, does not appear in Figure 2 because the **17** siloxane compounds present in VCPy, which collectively account for 0.29% of VCP emissions mass, each ranked outside the top 200. Nevertheless, the

chemical mechanisms developed for these VCP species may be useful and could account for larger fractions of emissions mass if different speciation profiles are used to characterize the composition of VCP emissions.

2.3. IVOC and SOA Formation

VCPy estimates emissions of compounds that are classified as intermediate volatility organic compounds (IVOC) because their volatility falls within the range 3×10^2 μg m^{-3} < C* < 3×10^6 μg m^{-3}, where C* is the saturation concentration [25]. CB6 lacks a model species for IVOC but many air quality models treat IVOC by implementing their own IVOC mechanism [21,22,30] to account for SOA production, e.g., CAMx includes the gas-phase reaction of IVOC with OH to produce SOA precursors without depleting OH such that IVOC emissions tend to increase SOA and have no impact on oxidants [22]. In the following analysis and discussion, we treat IVOC as a model species containing 15 carbons so that the mass of VCP emissions allocated to IVOC is obvious. We do not develop reaction mechanisms for IVOC to be compatible with model-specific treatments of IVOC. Similarly, the gas-phase mechanisms developed here do not include SOA formation because integration of oxidant with SOA chemistry schemes can be model-specific. Figure 1 may be helpful in coordinating implementation of our VCP oxidant mechanism with a specific SOA scheme.

2.4. Developing VCP Gas-Phase Chemical Mechanisms

Our VCP chemical mechanism is compatible with CB6 gas-phase mechanisms [19] including revision 3 (CB6r3) used in CMAQ [20,21] and CB6r5 used in CAMx [22] and will be compatible with CB7 revision 1 (CB7r1) to be available in CAMx in 2024. The VCP mechanism requires data for rate constants (k), which are obtained from (in order of preference) the IUPAC Task Group on Atmospheric Chemical Kinetic Data Evaluation [31], the NASA Panel for Data Evaluation [32], original published research, or the MCM [16]. The VCP mechanism also requires information on reaction mechanisms which we derived from (in order of preference) the MCM [16], published original research, or the SAPRC-07 chemical mechanism [33,34]. Although we did not explicitly rely upon data from the SAPRC-07 mechanism, we did review SAPRC-07 VCP reaction schemes, recognizing that the SAPRC-07 mechanism has been extensively evaluated against chamber experiments.

Rate constant variation with temperature for most VCP species is described by an Arrhenius expression, $k(T) = A \exp(-Ea/T)$, where A is the pre-exponential factor and Ea the activation energy (in Kelvin). Some VCP species use a modified Arrhenius expression, $k(T) = A\ T^2 \exp(-Ea/T)$, when available. We computed an average rate constant for lumped VCP species by averaging rate constants over contributing compounds. However, calculating a representative Ea is not straightforward because the contributing compounds may use a mix of Arrhenius and modified Arrhenius expressions and/or because averaging divergent Ea values weight the rate constants unequally. We determined Arrhenius expressions for lumped species as follows: compute the contributing rate constants at 283 K, 298 K and 313 K, average these values over the contributing compounds, compute the average Ea from the ratio of average rate constants at 283 K and 313 K, and finally compute the average A from the average Ea and the average rate constant at 298 K.

2.5. Ozone-Forming Tendency of VCP Model Species

The chemical mechanisms developed for VCPs were characterized by using MIR factors [27] to quantify OFP under atmospheric conditions where adding VOC emission yields the highest incremental increase in O_3 concentration (MIR condition). MIR values for VCP mechanism species were computed by applying CAMx as a box model for representative Los Angeles conditions and using the Decoupled Direct Method (DDM) in CAMx [35,36] to compute the sensitivity of the O_3 concentration to emissions of an individual VOC ($d[O_3]/d[VOC]$) which is proportional to the MIR. By definition, the MIR condition occurs under VOC-limited O_3 formation regimes where adding VOC has the greatest incremental

impact on the O_3 production rate and we adjusted the NOx emission input to the box model (holding VOC emissions constant) to maximize d[O_3]/d[VOC] and obtain MIR conditions. MIR values computed here are not identical to SAPRC MIR values [34] because the box model scenarios employed and chemical mechanisms differ. We computed MIR values for the purpose of evaluating the effects of mechanism updates (Section 3.6).

The CAMx box model domain has 3 × 3 × 2 grid cells (in the x, y, and z dimensions), which is the smallest allowable CAMx domain, since edge grid cells containing boundary conditions (BCs) are required by CAMx and 2 layers is the minimum allowed by the solution of vertical transport. All 9 grid cells in each layer have identical meteorological input data and a nominal 4 km grid size. The center grid cells of each domain, i.e., (2,2,1) and (2,2,2), form a 1-D column, with layer 1 representing the planetary boundary layer (PBL) and layer 2 representing a residual layer between the PBL and the CAMx top. Box model input data for 4 consecutive days were extracted from a full 3D simulation of California [37] with meteorology from the Weather Research and Forecasting (WRF) model version 3.8 (Figure S1) and emissions from a U.S. EPA 2011 emission inventory. The PBL depth varies in time, as modeled by WRF, whereas the top of layer 2 is constant in time at 3000 m. Horizontal wind speeds in layer 1 are set to zero, preventing horizontal exchange between grid cells and ensuring lateral BCs have no influence. In layer 2, there is a constant horizontal wind speed to purge the layer with a 12 h lifetime to limit the accumulation of pollutants over time. The box model simulation produced daily maximum 1 h O_3 around 120 ppb on three consecutive days (Figure S2).

3. Results and Discussion

The VCP mechanism introduces 19 mechanism species (Table 1) of which 16 are intended for representing VCP emissions. Our mechanism focuses on oxidant production and considers reactions with OH-radical reactions for a total of 25 reactions, listed in Table 2.

Table 2. The VCP chemical mechanism for use with CB6.

No.	Reaction	Rate Expression	k_{298}
R1	EDOH + OH = GLYD + HO2	$k = 1.45 \times 10^{-11}$	1.45×10^{-11}
R2	PDOH + OH = 0.61 ACET + 0.39 ALDX + 0.39 PAR + HO2	$k = 2.10 \times 10^{-11}$	2.10×10^{-11}
R3	IPOH + OH = 0.86 ACET + 0.14 ALD2 + 0.14 FORM + 0.86 HO2 + 0.14 XO2H + 0.14 RO2	$k = 2.60 \times 10^{-12}$ exp(200/T)	5.09×10^{-12}
R4	NPOH + OH = 0.55 ALDX + 0.43 ALD2 + 0.55 PAR + 0.43 FORM + 0.48 HO2 + 0.5 XO2H + 0.02 XO2N + 0.52 RO2	$k = 4.60 \times 10^{-12}$ exp(70/T)	5.82×10^{-12}
R5	ROH + OH = 0.2 ALDX + 2.71 PAR + 0.77 ROR + 0.2 HO2 + 0.77 XO2 + 0.03 XO2N + 0.8 RO2	$k = 7.00 \times 10^{-12}$ exp(60/T)	8.56×10^{-12}
R6	DME + OH = 0.99 MEFM + 0.99 XO2H + 0.01 XO2N + RO2	$k = 5.70 \times 10^{-12}$ exp(−215/T)	2.77×10^{-12}
R7	DEE + OH = 0.85 ETFM + 0.07 FORM + 0.85 MEO2 + 0.92 XO2 + 0.07 XO2H + 0.08 XO2N + 1.92 RO2	$k = 8.91 \times 10^{-18}$ T^2 exp(837/T)	1.31×10^{-11}
R8	ETHR + OH = 0.62 ESTR + 0.3 ALDX + 0.3 PAR + 0.62 MEO2 + 0.3 XO2H + 0.62 XO2 + 0.08 XO2N + RO2	$k = 8.90 \times 10^{-12}$ exp(100/T)	1.24×10^{-11}
R9	MEFM + OH = 0.17 FACD + 0.55 CO + 0.45 MEO2 + 0.55 XO2H + 0.005 XO2N + RO2	$k = 9.39 \times 10^{-13}$ exp(−461/T)	2.00×10^{-13}
R10	MEAC + OH = 0.67 AACD + 0.67 CO + 0.32 MEO2 + 0.67 XO2H + 0.32 XO2 + 0.01 XO2N + 1.32 RO2	$k = 8.54 \times 10^{-19}$ T^2 exp(455/T)	3.49×10^{-13}

Table 2. *Cont.*

No.	Reaction	Rate Expression	k_{298}
R11	ETFM + OH = 0.78 AACD + 0.78 CO + 0.2 ALD2 + 0.98 XO2H + 0.02 XO2N + 1.2 RO2	$k = 5.66 \times 10^{-13}$ exp(134/T)	8.87×10^{-13}
R12	ETAC + OH = 0.93 AACD + 0.93 C2O3 + 0.93 XO2 + 0.07 XO2N + RO2	$k = 6.92 \times 10^{-19}$ T^2 exp(986/T)	1.68×10^{-12}
R13	ESTR + OH = 0.13 AACD + 0.13 FACD + 1.9 PAR + 0.63 ROR + 0.25 CXO3 + 0.89 XO2 + 0.11 XO2N + RO2	$k = 2.50 \times 10^{-13}$exp(740/T)	2.99×10^{-12}
R14	SXD5 + OH = FORM + FACD + XO2H + RO2	$k = 2.10 \times 10^{-12}$	2.10×10^{-12}
R15	IBTA + OH = 0.78 ACET + 0.19 ALDX + 0.78 MEO2 + 0.78 XO2 + 0.19 XO2H + 0.03 XO2N + RO2	$k = 5.40 \times 10^{-12}$ exp(−285/T)	2.08×10^{-12}
R16	HPAR + OH = HPO2 + RO2	$k = 2.54 \times 10^{-11}$ exp(−180/T)	1.39×10^{-11}
R17	HPO2 + NO = NTR2	k = k(ref)/K k(ref) = k(RO2 + NO) $K = 9.09 \times 10^{2}$ exp(−1658/T)	2.59×10^{-12}
R18	HPO2 + NO = NO2 + HKET + AUTX	k = k(ref)/K k(ref) = k(RO2 + NO) $K = 1.43 \times 10^{-1}$ exp(679/T)	6.46×10^{-12}
R19	HPO2 + HO2 = ROOH + 0.5 HKET	k = k(ref)/K k(ref) = k(RO2 + HO2) K = 0.707	2.14×10^{-11}
R20	HPO2 + RO2 = 0.6 HKET + 0.6 AUTX + 0.6 RO2	k = k(ref)/K k(ref) = k(RO2 + RO2) K = 1.0	5.00×10^{-13}
R21	AUTX + NO = 0.82 NO2 + 0.82 HO2 + 0.18 NTR2	k = k(ref)/K k(ref) = k(RO2 + NO) K = 1.0	9.04×10^{-12}
R22	AUTX + HO2 = ROOH	k = k(ref)/K k(ref) = k(RO2 + HO2) K = 0.707	2.14×10^{-11}
R23	AUTX = ROOH + HO2	$k = 2.20 \times 10^{8}$ exp(−6200/T)	2.03×10^{-1}
R24	HKET + OH = 0.35 HKET + 0.35 KET + 0.47 ALDX + 0.7 HO2 + 0.24 XO2H + 0.07 XO2N + 0.3 RO2	$k = 1.50 \times 10^{-11}$	1.50×10^{-11}
R25	HKET = ALD2 + ALDX + CXO3 + XO2H + RO2	Photolysis	2.08×10^{-7}

k_{298} is the rate constant at 298 K and 1 atmosphere in units s^{-1} for 1st-order reactions or cm^3 $molecule^{-1}$ s^{-1} for 2nd-order reactions. The photolysis frequency (s^{-1}) of HKET in R25 is assumed to be the same as methyl ethyl ketone.

3.1. Alcohols

The CB6 mechanism explicitly represents two alcohols, namely methanol (MEOH) and ethanol (ETOH), and the VCP mechanism adds four explicit alcohols (EDOH, PDOH, IPOH and NPOH) and one lumped alcohol (ROH), as identified in Table 1. The reaction of EDOH with OH (R1 in Table 2) uses the rate constant recommended by IUPAC [31] in data sheet HOx_VOC71 with products directly from the MCM version 3.3.1 [16]. The MCM has only one reaction of 1,2-ethanediol that forms products which already exist in CB6 (glycolaldehyde and HO_2 radical), making the derivation of R1 straightforward.

The reaction of PDOH with OH uses the rate constant recommended by IUPAC (data sheet HOx_VOC73), with products derived from the MCM by condensing two

reactions of 1,2-propanediol to a single reaction (R2) by using the MCM branching ratio. Reaction at the 1-position of PDOH accounts for 39% of the total OH-reaction and forms propionaldehyde + HO_2, with propionaldehyde being represented in CB6 as ALDX + PAR. Reaction at the 2-position of PDOH accounts for 61% of the total OH-reaction and forms hydroxyacetone + HO_2, with hydroxyacetone represented here by ACET as a surrogate, although hydroxyacetone is an explicit species in CB7.

The OH reactions of IPOH (R3) and NPOH (R4) both use rate constants from the MCM and products derived from the MCM by combining reaction branches, as discussed for the OH-reaction with PDOH. The MCM scheme for 2-propanol (IPOH) has 136 reactions and 50 species (not counting inorganic reactions) and the scheme for 1-propanol (NPOH) has 199 reactions and 71 species, although some of these reactions are for organic species already included in CB6 such as acetaldehyde (ALD2) and formaldehyde (FORM). We developed condensed mechanisms for IPOH and NPOH from MCM schemes by focusing on the first-generation products of unimolecular RO_2 reactions and alkylperoxy radical (RO_2) reactions with NO, which are aldehydes and ketones for IPOH and NPOH, and representing RO_2 radical removal using CB6 mechanism species XO2, XO2H and/or XO2N. The species XO2 can represent the fate of many RO_2 radicals via reactions with NO to form NO_2, with HO_2 to form an organic peroxide (ROOH) or termination by reaction with any RO_2 radical. The species XO2H reacts like XO2 but also includes prompt HO_2 formation from NO-reaction. The species XO2N represents organic nitrate (ON) production from NO-reaction. Reactions R3 and R4 produce CB6 species RO2 which has the sole purpose of estimating the total RO2 radical concentration (i.e., summed over all different types of RO_2 species in CB6) to simplify representation of RO_2 + RO_2 termination reactions. Accordingly, the stoichiometric coefficient for RO2 in R3 and R4 equals the sum of coefficients for XO2, XO2H and XO2N.

The VCP mechanism species ROH represents alcohols other than the explicitly represented C1 to C3 alcohols, namely MEOH, ETOH, IPOH, NPOH, EDOH and PDOH. ROH is a lumped species containing four carbon atoms (Table 1) to allow mapping alcohols with four or more carbons (C4+) to ROH plus PAR as needed to conserve carbon, e.g., 1-hexanol maps to ROH + 2 PAR. The MCM contains nine alcohol compounds containing four or five carbons and the OH-reaction of ROH (R5) represents a weighted average of these nine alcohols with weighting factors that assume C4 alcohols are more abundant than C5 alcohols (60:40 split) and that 1-butanol is most abundant, as follows: 1-butanol (25%), 2-butanol (10%), i-butanol (20%), t-butanol (5%), 3-pentanol (8%), 2-methyl-1-butanol (8%), 3-methyl-1-butanol (8%), 2-methyl-2-butanol (8%), 3-methyl-2-butanol (8%). We analyzed the MCM scheme for each contributing alcohol using the approach summarized for IPOH and considering four product pathways: aldehyde + HO_2 radical; ketone + RO_2 radical represented by XO2H; alkoxy radical (represented by ROR) + RO_2 radical represented by XO2; and ON formation represented by XO2N. The CB6 species ROR represents the temperature-dependent conversion of alkoxy radicals from PAR to ketones and aldehydes (discussed in Section 3.4).

Previously, C3+ alcohols were most likely mapped to PAR when processing emission inventories for CB mechanisms [22]. The OH reactions of ROH and PAR form similar products (i.e., aldehydes and ketones) although ON formation is lower for ROH than PAR (3% compared to 13% at 298 K) and the OH-rate constant for ROH is faster than for the C-equivalent of 4 PAR (8.56×10^{-12} compared to 3.24×10^{-12} cm^3 $molecule^{-1}$ s^{-1} at 298 K).

3.2. Ethers

There are no explicit ether species in the CB6 mechanism and the VCP mechanism adds two explicit ethers (DME and DEE) and one lumped species to represent C4+ ethers (ETHR), as identified in Table 1. The reaction of DME with OH (R6) uses the rate constant recommended by IUPAC (data sheet HOx_VOC30), with products directly from the MCM. The MCM has only one OH-reaction for dimethyl ether with the dominant C-containing

product being methyl formate, which is included in the VCP mechanism as species MEFM. The OH-reaction of DEE (R7) uses the rate constant from MCM with products derived from the MCM using the condensation approach described above for IPOH and NPOH. The dominant C-containing product from DEE is ethyl formate (ETFM). Thus, reactions for DME and DEE depend on the presence of the reactions for MEFM and ETFM that are described below.

The VCP mechanism species ETHR is a lumped species containing four carbon atoms (Table 1) to allow mapping ethers with four or more carbons (other than DEE) to ETHR plus PAR as needed to conserve carbon, e.g., ethyl t-butyl ether maps to ETHR + 2 PAR. The top **200** VCP compounds analyzed for Figure 3 include 15 ethers, of which 11 also contain an alcohol group (ether–alcohol solvents such as 1-butoxy-2-propanol) and another 4 that also contain an ester group (ether-ester solvents such as 2-ethoxyethyl acetate). The MCM provides mechanisms for five ether-alcohol compounds. They form both esters (like DEE and DME) and aldehydes/ketones via alkoxy radical decomposition (like ROH) depending upon the ether-alcohol molecular structure and the location of initial OH-reaction. The ETHR reaction mechanism includes both product types and we recommend mapping ether–alcohol compounds to ETHR and PAR (not ROH and PAR), as illustrated in Table S2. The MCM does not include ether–ester compounds and we recommend mapping ether–esters to ETHR and PAR (not ESTR and PAR) because the derived OH-rate constant for ETHR is faster than for ESTR (Table 2), suggesting that OH-reaction at the ether group will predominate for these compounds.

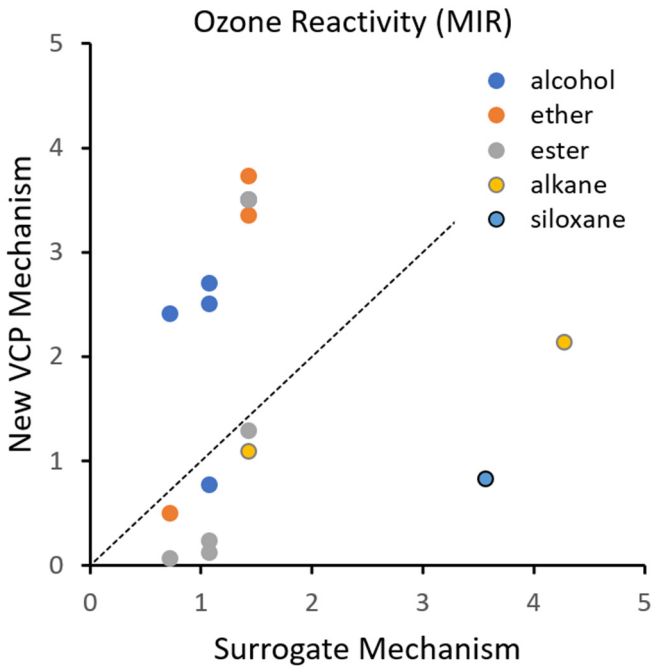

Figure 3. MIR factors (mole O_3/mole VOC) for VCP species in the new VCP mechanism compared to a "surrogate mechanism" approach of representing each VCP species using PAR. The dotted line indicates a 1:1 relationship.

The OH-reaction of ETHR (R8) is an unweighted average of mechanisms derived from MCM for 2-methoxy ethanol, 2-ethoxy ethanol, 2-butoxy ethanol, methyl t-butyl ether (MTBE) and ethyl t-butyl ether (ETBE). We analyzed the MCM scheme for each contributing ether using the approach summarized for IPOH and considering three product pathways: ester + RO_2 radical; aldehyde + RO_2 radical; and ON formation represented by XO2N. Including MTBE and ETBE in the derivation of the ETHR mechanism is important because they are added to some gasoline blends to improve octane-rating and therefore can be present in mobile source emissions.

Previously, ethers, ether–alcohols and ether–ester compounds were most likely mapped to PAR when processing emission inventories for CB mechanisms [22]. Mapping these compounds to ETHR rather than PAR produces esters that are not produced from PAR, reduces ON formation (8% compared to 13% at 298 K) and increases the OH-rate constant (1.24×10^{-11} for ETHR as compared to 3.24×10^{-12} cm^3 $molecule^{-1}$ s^{-1} for the C-equivalent of 4 PAR at 298 K).

3.3. Esters

There are no explicit ester species in the CB6 mechanism and the VCP mechanism adds four explicit esters (MEFM, ETFM, MEAC, ETAC) and one lumped compound to represent C4+ esters (ESTR), as identified in Table 1. The OH-reaction of MEFM (R9) uses the rate constant from MCM, with products derived by condensation from the 353 reactions of 128 species in MCM using the approach summarized for IPOH and NPOH. The products of R9 are consistent with those observed by Wallington et al. [38].

The OH-reaction of ETAC (R12) uses the rate constant from MCM with products based on the chamber experiments of Tuazon et al. [39], who discovered that the OH-reaction of ethyl acetate produces acetic acid (AACD in CB6) via a so-called "ester rearrangement" reaction. However, the MCM version 3.3.1 omits the ester rearrangement pathway for ethyl acetate. AACD is the dominant molecular product of R12 (93% yield) with acetyl peroxy radical (C2O3 in CB6) formed in equal amounts.

The OH-reaction of MEAC (R10) uses the rate constant from MCM with products based on the MCM but modified to reflect the expected importance of the ester rearrangement pathway [40]. The OH-reaction of ETFM (R11) uses the rate constant measured by LeCalve et al. [41], with products based on Szilágyi et al. [42] and by analogy with the mechanisms derived for MEFM and ETAC.

The VCP mechanism species ESTR is a lumped species containing four carbon atoms (Table 1) to allow mapping esters with four or more carbons to ESTR plus PAR as needed to conserve carbon, e.g., n-butyl acetate maps to ESTR + 2 PAR. Exceptions are representing ethyl acetate explicitly as ETAC, representing ether–esters as ETHR (discussed above) and representing large esters with low volatility as IVOC.

The rate constant for the OH-reaction of ESTR (R13) represents an average of seven esters included in MCM, namely n-propyl acetate, i-propyl acetate, n-butyl acetate, i-butyl acetate, s-butyl acetate, n-propyl formate and i-propyl formate. Products are based on the MCM schemes for the contributing esters adjusted to account for ester rearrangements and therefore considering four product pathways: formic acid (FACD) + acylperoxy radical (represented by CXO3) + RO_2 radical represented by XO2; acetic or larger acid represented by AACD + CXO3 + XO2; alkoxy radical represented by ROR + XO2; and ON formation represented by XO2N.

Previously, esters were most likely mapped to PAR when processing emission inventories for CB mechanisms [22]. Mapping compounds to ESTR rather than PAR directly produces carboxylic acids that are not directly produced from PAR, has little impact on ON formation (11% compared to 13% at 298 K) and has little impact on the OH-rate constant (2.99×10^{-12} for ESTR as compared to 3.24×10^{-12} cm^3 $molecule^{-1}$ s^{-1} for the C-equivalent of 4 PAR at 298 K).

3.4. Alkanes

Alkanes larger than propane are represented in CB6 by mechanism species PAR, which contains one carbon [17], such that butanes map to 4 PAR, pentanes map to 5 PAR, etc. The chemical mechanism for the OH-reaction of PAR in CB6r5 [22] is shown in Table 3. The species ROR represents alkoxy radicals formed from alkanes and their fate is determined by competition between unimolecular decomposition (P2) and O_2-reaction (P3), which depends on temperature and pressure. The species XPAR allows ON formation, represented by XO2N formed in reaction P5, to vary with temperature and pressure, as parameterized by Yeh and Ziemann [43]. The Yeh and Ziemann parameterization explicitly accounts for

the observed increase in ON yield with alkane size and the rate expression for P5 assumes that, on average, alkanes represented by PAR contain 5.5 carbons [17] producing a 13% ON yield from PAR (rate constant ratio P5/[P5 + P6]) at 298 K and 1 atmosphere.

Table 3. The PAR chemical mechanism from CB6r5.

No.	Reaction	Rate Expression	k_{298}
P1	PAR + OH = XPAR	$k = 8.10 \times 10^{-13}$	8.10×10^{-13}
P2	ROR = 0.2 KET + 0.42 ACET + 0.74 ALD2 + 0.37 ALDX + 0.04 XO2N + 0.94 XO2H + 0.98 RO2 + 0.02 ROR − 2.7 PAR	$k = 5.70 \times 10^{12}$ exp(−5780/T)	2.15×10^{4}
P3	ROR + O2 = KET + HO2	$k = 1.50 \times 10^{-14}$ exp(−200/T)	7.67×10^{-15}
P4	ROR + NO2 = NTR1	$k = 8.60 \times 10^{-12}$ exp(400/T)	3.29×10^{-11}
P5	XPAR = XO2N + RO2	Falloff: F = 0.41; n = 1 k(0) = 4.81×10^{-20} k(inf) = 4.30×10^{-1} $(T/298)^{-8}$	1.49×10^{-1}
P6	XPAR = 0.126 ALDX + 0.874 ROR + 0.126 XO2H + 0.874 XO2 + RO2 − 0.126 PAR	k = 1.0	1.0

k_{298} is the rate constant at 298 K and 1 atmosphere in units s^{-1} for 1st-order reactions or cm^3 $molecule^{-1}$ s^{-1} for 2nd-order reactions. Falloff expression P5 depends on T and P and is evaluated as described by IUPAC [31].

The VCP mechanism adds one explicit alkane (IBTA) and one lumped alkane (HPAR), as identified in Table 1. The OH-reaction of IBTA (R15) uses the rate constant from IUPAC (data sheet HOx_VOC60) and products derived from the MCM using the condensation approach described above for IPOH and NPOH. The dominant C-containing product in R15 is acetone, formed in a higher yield from IBTA (78%) than from PAR (at most 42%). Methylperoxy radical (MEO2) also has 78% yield from IBTA and MEO2 is a precursor to formaldehyde. These differences in products between IBTA and PAR, combined with the prevalence of IBTA in VCP emissions (Figure 2), justify making IBTA an explicit species rather than representing isobutane as 4 PAR [22].

The reactions of HPAR (R16 to R25) represent large alkanes and the reaction scheme is based on the MCM mechanism for n-dodecane with adjustments to account for RO_2-radical autoxidation, which is important for larger alkanes [44] but omitted by the current version of MCM (v3.3.1). The rate constant for the OH-reaction of HPAR is from MCM for n-dodecane but using the temperature dependence (Ea) for n-decane because no temperature dependence is given for n-dodecane in the MCM. The alkylperoxy radical HPO2 produced in R15 can react with NO in R16 to form an ON (represented by the CB6 species NTR2 for larger ONs) or in R17 to produce an alkoxy radical. The rate constants for R16 and R17 are fitted to the temperature-dependent parameterization of Yeh and Ziemann [43] for n-dodecane, assuming 1 atmosphere pressure (this assumption adds little uncertainty because the pressure dependence of the ON-yield for n-dodecane is small). The alkoxy radical formed by R17 promptly isomerizes and adds O_2 to produce a hydroxy-alkylperoxy radical, which has the potential to further autoxidize, i.e., undergo isomerization followed by O_2 addition [44]. Potential autoxidation following R17 is represented by producing species AUTX (consumed by R21 to R23) together with products that would be the same with or without autoxidation (NO2 + HKET). The AUTX scheme has advantages for future development, which are discussed below. Autoxidation in R23 is based on a 1,6 H-shift, as shown by Praske et al. [44], which adds one hydroperoxyl functional group (represented by ROOH) and produces a HO_2 radical. Autoxidation is suppressed by the hydroxy-alkylperoxy radical reaction with HO_2 (R22) or NO (R21) to form conventional products. Reactions R21, R22 and R23 compete with each other: at 298 K, autoxidation (R23) will outcompete the NO-reaction (R21) when NO falls below ~1 ppb and the HO_2-reaction (R22)

is not competitive. However, the HO_2-reaction (R22) becomes more competitive for cold conditions (below ~273 K) because R21 has a strong temperature dependence. Reaction R20 of HPO2 with the total pool of RO_2 radicals (species RO2) is unlikely to be competitive with other reactions of HPO2 but nevertheless is included to ensure mechanism stability (i.e., to prevent the unconstrained accumulation of HPO2), assuming the 60% conversion of HPO2 to an alkoxy radical (based on MCM) and the remaining carbon-containing products being implicitly lost to aerosol formation.

Rate constants for the reactions of HPO2 and AUTX are referenced to standard CB6 reaction rates for RO_2 radical reactions with NO ($k = 2.40 \times 10^{-12} \exp(360/T)$) and HO_2 ($k = 4.80 \times 10^{-13} \exp(800/T)$) for consistency and to simply future mechanism updates (CB7). The ON yield from the HPO2 reaction with NO [k17/(k17 + k18)] is 28% at 298 K, in agreement with Yeh and Ziemann [43], but smaller than the ON yield from n-dodecane of 44% in the MCM, which is temperature-invariant in contrast to the HPO2 scheme. The additional 18% ON yield in R18 represents hydroxynitrate formation and is based on the MCM mechanism for n-dodecane.

The major carbon-containing products from HPO2 are all represented by the lumped species KHET, which is considered to be a hydroxy-peroxyketone (called a ketohydroperoxide by Praske et al.) produced by the autoxidation of HPO2. This species is not present in the MCM but a related hydroxyketone (MCM species HO5CO8C10 with SMILES structure CCCCC(O)CCC(=O)CC) has 901 reactions of 295 species that are characterized by fragmentation of the carbon backbone, producing aldehydes and retaining the ketone to some extent. The OH-rate constant for HKET in R24 is based on similar compounds in the MCM and the photolysis frequency (s^{-1}) of HKET in R25 is assumed to be the same as methyl ethyl ketone following the MCM. The OH-reaction of HKET is recursive, i.e., HKET is produced in R24, to approximate successive fragmentation reactions, and accordingly HKET is modeled as an eight-carbon species. We recommend against using HKET to represent emitted compounds because it is highly functionalized.

The autoxidation scheme using AUTX (R21 to R23) has potential for further development. As implemented, AUTX allows at most one autoxidation step (1,6 H-shift) but long alkyl chains can potentially undergo sequential autoxidation steps, which could be represented by increasing the yield of ROOH in R23. AUTX could be used to represent the autoxidation of other compounds, provided that the rate constants for autoxidation and competing reactions are comparable to those in R21 to R23.

HPAR is intended to represent larger alkanes, which requires coordinating how compounds are mapped to HPAR, PAR and, if present in the host model, IVOC. We recommend using PAR to represent alkanes containing 8 or less carbons and IVOC to represent alkanes containing 15 or more carbons and interpolating between these limits to avoid discontinuities, as shown in Table 4 and applied in Table S2. Table 4 mappings conserve carbon and are compatible with CAMx in which the IVOC species for anthropogenic emissions contains 15 carbons (see Section 2.3). Table 4 could be adapted for other models that adopt different treatments for IVOC.

Table 4. Recommended mechanism mappings for C9 to C14 alkanes.

Alkane	PAR (1 Carbon)	HPAR (12 Carbons)	IVOC (15 Carbons)	Total Carbon for PAR + HPAR + IVOC
C9	6	0.25		9
C10	4	0.5		10
C11	2	0.75		11
C12		1		12
C13		0.67	0.33	13
C14		0.33	0.67	14

3.5. Siloxanes

The VCP mechanism includes one lumped siloxane species (SXD5) based on decamethylcyclopentasiloxane (D5). The rate constant for the OH-reaction of SXD5 (R14) adopts the value for D5 measured by Alton and Browne [45]. The reaction mechanisms of siloxanes are poorly understood [46], with current mechanisms unable to fully explain products that are observed. The formation of formaldehyde and formic acid in R14 is near the middle of the range of yields measured by Kang et al. [47]. Implicitly, R14 assumes that most of the mass from reacted SXD5 is unreactive and potentially condensed to the aerosol phase [46,47].

3.6. Ozone Formation Potential of VCPs

We calculated MIR values (mole O_3/mole VOC) for each VCP species, and for the CB6 species PAR, using DDM sensitivity analysis within a CAMx box model for Los Angeles under strongly VOC-limited conditions (Table 5). These explicit MIR factors are compared in Figure 3 and Table 5 to an alternative "surrogate mechanism" approach of mapping the VCP species to PAR (e.g., IBTA maps to 4 PAR), which is a likely current practice [22].

Table 5. VCP species MIR factors (mole O_3/mole VOC) compared to MIR obtained by mapping the VCP to PAR.

VCP Species	MIR (Mole O_3/mole)	PAR Mapping	PAR MIR (Mole O_3/mole)	MIR Ratio (VCP/PAR)
IPOH	0.778	3	1.068	0.73
NPOH	2.707	3	1.068	2.53
EDOH	2.413	2	0.712	3.39
PDOH	2.508	3	1.068	2.35
ROH	3.506	4	1.424	2.46
DME	0.499	2	0.712	0.70
DEE	3.363	4	1.424	2.36
ETHR	3.735	4	1.424	2.62
MEFM	0.068	2	0.712	0.10
ETFM	0.237	3	1.068	0.22
MEAC	0.119	3	1.068	0.11
ETAC	3.506	4	1.424	2.46
ESTR	1.293	4	1.424	0.91
IBTA	1.091	4	1.424	0.77
HPAR	2.137	12	4.272	0.50
HKET	3.625	8	2.848	1.27
SXD5	0.828	10	3.56	0.23

PAR mapping is the number of carbons excluding any C(O)O ester group. PAR MIR = PAR mapping X 0.356 mole O_3/mole PAR.

For alcohols except IPOH, the VCP mechanism is more reactive (larger MIR) than the PAR equivalent by factors of 2.35 to 3.39, which is attributable to the alcohol group promoting the OH-reaction, i.e., increasing the OH rate constant. IPOH is less reactive than its PAR equivalent (ratio 0.73) because the dominant reaction product, acetone, is unreactive toward OH. For ethers except DME, the VCP mechanism is more reactive than the PAR equivalent by factors of 2.36 to 2.62, which is attributable to the ether group promoting the OH-reaction. DME is less reactive than its PAR equivalent (ratio 0.7) because the dominant reaction product, ethyl formate, is unreactive. Esters, except ETAC, are less reactive than the PAR equivalent (ratio 0.1 to 0.91) because their carboxylic acid reaction products (FACD

and AACD) are unreactive towards OH. ETAC is the only ester species more reactive than the PAR equivalent (ratio 2.46) because of a high yield (93%) of peroxyacetyl radical (C2O3), which is based on experimental data. IBTA is less reactive than the PAR equivalent (ratio 0.77) because the dominant reaction product, acetone, is unreactive toward OH. HPAR is less reactive than the PAR equivalent (ratio 0.5) in part because of the greater ON yield from HPAR than from PAR (28% compared to 13%). The lumped siloxane species SXD5 is much less reactive than the PAR equivalent (ratio 0.23) because the majority of the reaction products are considered unreactive by mechanisms based on current knowledge, which are uncertain as discussed above. MIR values for siloxanes in SAPRC-07 mechanisms are negative [34], indicating that siloxanes suppress ozone formation under MIR conditions, which reinforces the idea that siloxane reaction mechanisms are uncertain and can benefit from continued research.

4. Conclusions

We analyzed a 2019 VCP emission inventory for the U.S. [9] and found that ~67% of the emissions mass can be well-represented by existing CB6 mechanism species but ~33% could be better represented by adding VCP mechanism species to CB6. We identified 16 VCP mechanism species (11 explicit and 5 lumped) for addition in our gas-phase VCP mechanism, including alcohols, ethers, esters, alkanes and siloxanes. The resulting VCP chemical mechanism has 19 species and 25 reactions and is compatible with CB6 mechanisms in the current CAMx v7.2 [22] and CMAQ v5.3 [21] air quality models and will be incorporated into CB7.

We characterized the OFP of the added VCP mechanism species by computing MIR factors which quantify OFP for strongly VOC-limited conditions. The computed VCP MIR factors were compared to an alternative of mapping the VCP compound to the CB6 species PAR (representing paraffinic carbon), which is a likely current practice [22]. Nine of the sixteen added VCP species are less reactive (i.e., smaller MIR) than their PAR equivalents, namely i-propanol, dimethyl ether, methyl formate, ethyl formate, methyl acetate, larger esters, i-butane, large alkanes and lumped siloxanes. These less reactive VCP species are characterized by OH-reactions that form un-reactive products, such as acetone or carboxylic acids. Seven of the sixteen VCP species are more reactive than their PAR equivalents, namely n-propanol, ethylene glycol, propylene glycol, larger alcohols, diethyl ether, larger ethers and ethyl acetate. These more-reactive VCP species are characterized by containing a functional group that promotes faster OH-reaction (alcohol or ether group) or, in the case of ethyl acetate, by forming a highly reactive product.

The VCP chemical mechanism for CB6 can improve how VCP impacts O_3 and oxidants are represented by photochemical models. However, changes in oxidant formation due to the mechanism updates will depend on how VCP emissions are speciated for modeling, which is uncertain, and impacts may go in opposite directions for specific categories of VCP emissions that have unique chemical speciation characteristics. Better resolving the chemical speciation of VCPs for modeling can also support improved organic aerosol modeling; e.g., the large alkanes represented by HPAR tend to have larger SOA-yields than remaining alkanes represented by PAR. The chemical mechanism developed for HPAR explicitly includes temperature-dependent ON yields [43] and represents autoxidation by 1,6 H-shift reactions [44], consistent with current knowledge.

Supplementary Materials: The following supporting information can be downloaded at: https://www.mdpi.com/article/10.3390/atmos15020178/s1, Figure S1: Meteorological conditions for the Los Angeles box model scenario, shown in local standard time for 29 July to 2 August 2011; Figure S2: Time series for O_3, NO and NO_2 in the Los Angeles box model scenario, shown in local standard time for 29 July to 2 August 2011; Table S1: The top **39** compounds identified by ranking MIR- and SOA-weighted emissions in the VCPy 2019 U.S.-wide emission inventory. The percentage of emissions, MIR or SOA for each compound is the contribution to that sum over all compounds. The entry for CB6 (Yes or No) indicates whether the compound is considered well-represented by the mechanism species of CB6r5 and CB6r3. C* is the saturation vapor pressure in $\mu g\ m^{-3}$; Table S2:

Mapping compounds present in VCPy and SPECIATE to the VCP and CB6 mechanism species; Table S3: Emissions of CB6 species for the for the Los Angeles box model scenario on 31 July 2011, in moles/day/km^2.

Author Contributions: Conceptualization, G.Y.; methodology, G.Y. and K.T.; software, G.Y.; validation, G.Y.; formal analysis, G.Y. and K.T.; investigation, G.Y. and K.T.; resources, G.Y.; data curation, G.Y. and K.T.; writing—original draft preparation, G.Y. and K.T.; writing—review and editing, G.Y. and K.T.; visualization, G.Y. and K.T.; supervision, G.Y.; project administration, G.Y. and K.T.; funding acquisition, G.Y. All authors have read and agreed to the published version of the manuscript.

Funding: This research was supported by the Electric Power Research Institute (EPRI).

Institutional Review Board Statement: Not applicable.

Informed Consent Statement: Not applicable.

Data Availability Statement: Data are provided in the manuscript and Supplementary Material.

Acknowledgments: The authors acknowledge the support of EPRI and valuable discussions with Eladio Knipping of EPRI.

Conflicts of Interest: The authors declare no conflicts of interest. The funders had no role in the design of the study; in the collection, analyses, or interpretation of data; in the writing of the manuscript. The funders supported publishing the results.

References

1. Finlayson-Pitts, B.J.; Pitts, J.N., Jr. *Chemistry of the Upper and Lower Atmosphere: Theory, Experiments, and Applications*; Elsevier: Amsterdam, The Netherlands, 1999.
2. Lelieveld, J.; Evans, J.S.; Fnais, M.; Giannadaki, D.; Pozzer, A. The contribution of outdoor air pollution sources to premature mortality on a global scale. *Nature* **2015**, *525*, 367–371. [CrossRef]
3. Piccot, S.D.; Watson, J.J.; Jones, J.W. A global inventory of volatile organic compound emissions from anthropogenic sources. *J. Geophys. Res. Atmos.* **1992**, *97*, 9897–9912. [CrossRef]
4. Li, J.; Hao, Y.; Simayi, M.; Shi, Y.; Xi, Z.; Xie, S. Verification of anthropogenic VOC emission inventory through ambient measurements and satellite retrievals. *Atmos. Chem. Phys.* **2019**, *19*, 5905–5921. [CrossRef]
5. U. S. Environmental Protection Agency. Technical Support Document (TSD): Preparation of Emissions Inventories for the 2020 North American Emissions Modeling Platform, EPA-454/B-23-004, Research Triangle Park, NC. Available online: https://www.epa.gov/system/files/documents/2023-03/2016v3_EmisMod_TSD_January2023_1.pdf (accessed on 25 January 2024).
6. McDonald, B.C.; De Gouw, J.A.; Gilman, J.B.; Jathar, S.H.; Akherati, A.; Cappa, C.D.; Jimenez, J.L.; Lee-Taylor, J.; Hayes, P.L.; McKeen, S.A.; et al. Volatile chemical products emerging as largest petrochemical source of urban organic emissions. *Science* **2018**, *359*, 760–764. [CrossRef] [PubMed]
7. Khare, P.; Gentner, D.R. Considering the future of anthropogenic gas-phase organic compound emissions and the increasing influence of non-combustion sources on urban air quality. *Atmos. Chem. Phys.* **2018**, *18*, 5391–5413. [CrossRef]
8. Luo, D.; Corey, R.; Propper, R.; Collins, J.; Komorniczak, A.; Davis, M.; Berger, N.; Lum, S. Comprehensive environmental impact assessment of exempt volatile organic compounds in California. *Environ. Sci. Policy* **2011**, *14*, 585–593. [CrossRef]
9. Seltzer, K.M.; Murphy, B.N.; Pennington, E.A.; Allen, C.; Talgo, K.; Pye, H.O. Volatile chemical product enhancements to criteria pollutants in the United States. *Environ. Sci. Technol.* **2021**, *56*, 6905–6913. [CrossRef]
10. Sasidharan, S.; He, Y.; Akherati, A.; Li, Q.; Li, W.; Cocker, D.; McDonald, B.C.; Coggon, M.M.; Seltzer, K.M.; Pye, H.O.; et al. Secondary Organic Aerosol Formation from Volatile Chemical Product Emissions: Model Parameters and Contributions to Anthropogenic Aerosol. *Environ. Sci. Technol.* **2023**, *57*, 11891–11902. [CrossRef]
11. Emery, C.; Liu, Z.; Russell, A.G.; Odman, M.T.; Yarwood, G.; Kumar, N. Recommendations on statistics and benchmarks to assess photochemical model performance. *J. Air Waste Manag. Assoc.* **2017**, *67*, 582–598. [CrossRef]
12. Huang, L.; Zhu, Y.; Zhai, H.; Xue, S.; Zhu, T.; Shao, Y.; Liu, Z.; Emery, C.; Yarwood, G.; Wang, Y.; et al. Recommendations on benchmarks for numerical air quality model applications in China–Part 1: PM 2.5 and chemical species. *Atmos. Chem. Phys.* **2021**, *21*, 2725–2743. [CrossRef]
13. Belis, C.A.; Pirovano, G.; Villani, M.G.; Calori, G.; Pepe, N.; Putaud, J.P. Comparison of source apportionment approaches and analysis of non-linearity in a real case model application. *Geosci. Model Dev.* **2021**, *14*, 4731–4750. [CrossRef]
14. Levy, H. Normal atmosphere: Large radical and formaldehyde concentrations predicted. *Science* **1971**, *173*, 141–143. [CrossRef] [PubMed]
15. Kaduwela, A.; Luecken, D.; Carter, W.; Derwent, R. New directions: Atmospheric chemical mechanisms for the future. *Atmos. Environ.* **2015**, *122*, 609–610. [CrossRef]
16. Master Chemical Mechanism (v3.3.1). Available online: https://mcm.york.ac.uk/MCM/ (accessed on 22 December 2023).

17. Gery, M.W.; Whitten, G.Z.; Killus, J.P.; Dodge, M.C. A photochemical kinetics mechanism for urban and regional scale computer modeling. *J. Geophys. Res. Atmos.* **1989**, *94*, 12925–12956. [CrossRef]
18. Whitten, G.Z.; Heo, G.; Kimura, Y.; McDonald-Buller, E.; Allen, D.T.; Carter, W.P.; Yarwood, G. A new condensed toluene mechanism for Carbon Bond: CB05-TU. *Atmos. Environ.* **2010**, *44*, 5346–5355. [CrossRef]
19. Yarwood, G.; Jung, J.; Whitten, G.Z.; Heo, G.; Mellberg, J.; Estes, M. Updates to the Carbon Bond mechanism for version 6 (CB6). In Proceedings of the 9th Annual CMAS Conference, Chapel Hill, NC, USA, 11–13 October 2010; Available online: https://cmascenter.org/conference/2010/abstracts/emery_updates_carbon_2010.pdf (accessed on 22 December 2023).
20. Luecken, D.J.; Yarwood, G.; Hutzell, W.T. Multipollutant modeling of ozone, reactive nitrogen and HAPs across the continental US with CMAQ-CB6. *Atmos. Environ.* **2019**, *201*, 62–72. [CrossRef] [PubMed]
21. Appel, K.W.; Bash, J.O.; Fahey, K.M.; Foley, K.M.; Gilliam, R.C.; Hogrefe, C.; Hutzell, W.T.; Kang, D.; Mathur, R.; Murphy, B.N.; et al. The Community Multiscale Air Quality (CMAQ) model versions 5.3 and 5.3. 1: System updates and evaluation. *Geosci. Model Dev.* **2021**, *14*, 2867–2897. [CrossRef]
22. Ramboll. User Guide Comprehensive Air Quality Model with Extensions, Version 7.2. 2022. Available online: www.camx.com (accessed on 22 December 2023).
23. Manders, A.M.; Builtjes, P.J.; Curier, L.; Denier van der Gon, H.A.; Hendriks, C.; Jonkers, S.; Kranenburg, R.; Kuenen, J.J.; Segers, A.J.; Timmermans, R.M.; et al. Curriculum vitae of the LOTOS–EUROS (v2. 0) chemistry transport model. *Geosci. Model Dev.* **2017**, *10*, 4145–4173. [CrossRef]
24. Wolfe, G.M.; Marvin, M.R.; Roberts, S.J.; Travis, K.R.; Liao, J. The framework for 0-D atmospheric modeling (F0AM) v3. 1. *Geosci. Model Dev.* **2016**, *9*, 3309–3319. [CrossRef]
25. Seltzer, K.M.; Pennington, E.; Rao, V.; Murphy, B.N.; Strum, M.; Isaacs, K.K.; Pye, H.O. Reactive organic carbon emissions from volatile chemical products. *Atmos. Chem. Phys.* **2021**, *21*, 5079–5100. [CrossRef]
26. Ramboll. Speciation Tool User's Guide, version 5.0. 2020. Available online: https://github.com/CMASCenter/Speciation-Tool/blob/master/docs/Ramboll_sptool_users_guide_V5.pdf (accessed on 22 December 2023).
27. Carter, W.P. Development of ozone reactivity scales for volatile organic compounds. *Air Waste* **1994**, *44*, 881–899. [CrossRef]
28. U. S. Environmental Protection Agency. Final Report, SPECIATE Version 5.0, Database Development Documentation, EPA/600/R-19/988, Research Triangle Park, NC. Available online: https://www.epa.gov/air-emissions-modeling/speciate-51-and-50-addendum-and-final-report (accessed on 22 December 2023).
29. Carter, W.P.L. Updated Maximum Incremental Reactivity Scale and Hydrocarbon Bin Reactivities for Regulatory Applications, Prepared for California Air Resources Board Contract 07-339. Available online: https://intra.engr.ucr.edu/~carter/SAPRC/MIR10.pdf (accessed on 22 December 2023).
30. Huang, L.; Liu, H.; Yarwood, G.; Wilson, G.; Tao, J.; Han, Z.; Ji, D.; Wang, Y.; Li, L. Modeling of secondary organic aerosols (SOA) based on two commonly used air quality models in China: Consistent S/IVOCs contribution but large differences in SOA aging. *Sci. Total Environ.* **2023**, *903*, 166162. [CrossRef]
31. IUPAC Task Group on Atmospheric Chemical Kinetic Data Evaluation, Evaluated kinetic data. Available online: https://iupac.aeris-data.fr/en/home-english/ (accessed on 22 December 2023).
32. NASA Chemical Kinetics and Photochemical Data for Use in Atmospheric Studies, Panel for Data Evaluation, JPL Publication No. 19-5. Available online: https://jpldataeval.jpl.nasa.gov/pdf/NASA-JPL%20Evaluation%2019-5.pdf (accessed on 22 December 2023).
33. Carter, W.P.L. Development of the SAPRC-07 chemical mechanism. *Atmos. Environ.* **2010**, *44*, 324–5335. [CrossRef]
34. Carter, W.P. Development of the SAPRC-07 Chemical Mechanism and Updated Ozone Reactivity Scales. California Air Resources Board, Research Division. 2007. Available online: https://intra.engr.ucr.edu/~carter/SAPRC/saprc07.pdf (accessed on 25 January 2024).
35. Dunker, A.M. The decoupled direct method for calculating sensitivity coefficients in chemical kinetics. *J. Chem. Phys.* **1984**, *81*, 2385–2393. [CrossRef]
36. Dunker, A.M.; Yarwood, G.; Ortmann, J.P.; Wilson, G.M. Comparison of source apportionment and source sensitivity of ozone in a three-dimensional air quality model. *Environ. Sci. Technol.* **2002**, *36*, 2953–2964. [CrossRef]
37. California Energy Commission. Air Quality Implications of an Energy Scenario for California Using High Levels of Electrification, report CEC-500-2019-049. Available online: https://www.energy.ca.gov/sites/default/files/2021-06/CEC-500-2019-049.pdf (accessed on 22 December 2023).
38. Wallington, T.J.; Hurley, M.D.; Maurer, T.; Barnes, I.; Becker, K.H.; Tyndall, G.S.; Orlando, J.J.; Pimentel, A.S.; Bilde, M. Atmospheric oxidation mechanism of methyl formate. *J. Phys. Chem. A* **2001**, *105*, 5146–5154. [CrossRef]
39. Tuazon, E.C.; Aschmann, S.M.; Atkinson, R.; Carter, W.P. The Reactions of Selected Acetates with the OH Radical in the Presence of NO: Novel Rearrangement of Alkoxy Radicals of Structure RC (O) OCH (Ȯ) Ŕ. *J. Phys. Chem. A* **1998**, *102*, 2316–2321. [CrossRef]
40. Orlando, J.J.; Tyndall, G.S.; Wallington, T.J. The atmospheric chemistry of alkoxy radicals. *Chem. Rev.* **2003**, *103*, 4657–4690. [CrossRef] [PubMed]
41. Le Calve, S.; Le Bras, G.; Mellouki, A. Temperature dependence for the rate coefficients of the reactions of the OH radical with a series of formates. *J. Phys. Chem. A* **1997**, *101*, 5489–5493. [CrossRef]
42. Szilágyi, I.; Dóbé, S.; Bérces, T.; Márta, F.; Viskolcz, B. Direct kinetic study of reactions of hydroxyl radicals with alkyl formates. *Z. Für Phys. Chem.* **2004**, *218*, 479–492. [CrossRef]

43. Yeh, G.K.; Ziemann, P.J. Alkyl nitrate formation from the reactions of c8–c14 n-alkanes with oh radicals in the presence of no x: Measured yields with essential corrections for gas–wall partitioning. *J. Phys. Chem. A* **2014**, *118*, 8147–8157. [CrossRef] [PubMed]
44. Praske, E.; Otkjær, R.V.; Crounse, J.D.; Hethcox, J.C.; Stoltz, B.M.; Kjaergaard, H.G.; Wennberg, P.O. Atmospheric autoxidation is increasingly important in urban and suburban North America. *Proc. Natl. Acad. Sci. USA* **2018**, *115*, 64–69. [CrossRef] [PubMed]
45. Alton, M.W.; Browne, E.C. Atmospheric chemistry of volatile methyl siloxanes: Kinetics and products of oxidation by OH radicals and Cl atoms. *Environ. Sci. Technol.* **2020**, *54*, 5992–5999. [CrossRef] [PubMed]
46. Alton, M.W.; Johnson, V.L.; Sharma, S.; Browne, E.C. Volatile Methyl Siloxane Atmospheric Oxidation Mechanism from a Theoretical Perspective—How is the Siloxanol Formed? *J. Phys. Chem. A* **2023**, *127*, 10233–10242. [CrossRef]
47. Kang, H.G.; Chen, Y.; Park, Y.; Berkemeier, T.; Kim, H. Volatile oxidation products and secondary organosiloxane aerosol from D 5+ OH at varying OH exposures. *Atmos. Chem. Phys.* **2023**, *23*, 14307–14323. [CrossRef]